Scientia Iranica D (2023) 30(4), 1296–1313

Sharif University of Technology
Scientia Iranica
Transactions D: Computer Science & Engineering and Electrical Engineering
http://scientiairanica.sharif.edu

Residential demand response coordination for distribution network reliability enhancement

M. Kabirifar, M. Fotuhi-Firuzabad*, and A. Safdarian

Department of Electrical Engineering, Center of Excellence in Power System Control and Management, Sharif University of Technology, Tehran, Iran.

Received 13 November 2020; received in revised form 22 July 2021; accepted 8 November 2021

KEYWORDS
Centralized model;
Demand response;
Distribution system operator;
Reliability;
Responsive appliances.

Abstract. This paper proposes a centralized model to activate a residential demand response to improve the reliability of a distribution network. The model aims to minimize the damage cost imposed by load curtailments following the occurrence of unexpected events. In this model, the Distribution System Operator (DSO) and responsive customers have already signed a contract authorizing the DSO to alter the operation of responsive appliances in case system reliability is jeopardized. The model addresses consumers' preferences and guarantees that the operation of appliances be displaced within the bounds defined by the owners. Once an unexpected event occurs, the DSO commits responsive appliances to avoid likely violations in the network operational limits and costly load curtailments. The proposed model is mathematically formulated in the form of Mixed Integer Linear Programming (MILP) and its capability is depicted via applying to a real-world distribution network with some residential consumers. The comparison of service reliability indices after and before utilizing demand response potentials illustrates the effectiveness of the model.

1. Introduction

The reliability of electricity infrastructure plays a pivotal role in driving forces towards the prosperity of modern societies. However, electricity networks are susceptible to a broad range of faults. The faults followed by unexpected service disruptions may paralyze the industry, agriculture, and even residential sector, thereby imposing huge damage costs on the society [1]. The high costs associated with unreliable electricity services have long been a significant motivating factor for area experts, engineers, and researchers to seek out solutions to improve the reliability of electricity services. In power systems, faults in distribution networks account for almost 80% of all reliability issues. This implies that distribution networks, which have historically received less attention, are the most suitable option to focus on when the goal is to improve the reliability of electricity services.

So far, many solutions have been proposed to enhance service reliability of distribution networks, such as regular maintenance activities [2], local generation [3], and Demand Response (DR) [4], to name just

*. *Corresponding author. Tel.: +98 21 66164040;*
E-mail addresses: milad.kabirifar@ee.sharif.edu (M. Kabirifar); fotuhi@sharif.edu (M. Fotuhi-Firuzabad); safdarian@sharif.edu (A. Safdarian)

doi: 10.24200/sci.2021.57163.5095

a few. This paper primarily focuses on the third solution, which involves utilizing demand flexibility to enhance the reliability of electricity services. In 2012, the envisioned reliability advantages of DR persuaded the North American Electric Reliability Corporation (NERC) to establish a system for regular data collection and a semi-annual report to announce and measure the contribution of DR to service reliability issues [5]. Despite its significance, only a limited number of studies have quantified DR benefits for enhancing service reliability and attempted to develop models to achieve these benefits. A large producer of aluminum products and its DR capability to serve reliability services were studied in [6]. While valuable, this study focused on a single customer with specific characteristics, and the results may not be generalizable to other consumers. The research presented in [7] estimated the minimum amount of load reduction required to prevent voltage collapse. Accounting for the flexibility of demand, the study conducted in [8] estimated the cost of customer interruptions resulting from unforeseen service outages. The obtained results demonstrated that DR could effectively reduce interruption costs, especially in the case of short-duration interruptions. In [9], the system load profile was adjusted based on the wholesale market prices, and a number of reliability indices were computed and compared before and after the modification. The provided results highlight the significant role that DR can play in enhancing reliability. In [10], impacts of DR on distribution network reliability were qualitatively studied. The study lacked a quantitative analysis, which is essential to substantiate the drawn conclusions. A quantitative study, along with sensitivity analyses, was conducted in a study referenced in [11], addressing the aforementioned issue and demonstrating the significant benefits of DR to distribution network reliability. Furthermore, authors in [12] investigated the role of commercial DR in the reliability of a technical virtual power plant.

The literature mentioned above primarily concentrates on the impact of DR on network reliability. However, it has also been demonstrated that the coordination of responses from residential customers is crucial to achieve the maximum envisioned benefits. Research has indicated that autonomous responses from residential consumers could result in significant peak rebounds, which may lead to violations of distribution network constraints [13]. Therefore, system-wide frameworks are required to coordinate responses from different consumers so that the overall system efficiency and reliability can be enhanced. In [14,15], time-varying prices were designed to ensure that potential negative impacts were avoided. In [16–20], algorithms were introduced to coordinate consumers' DR activities. These algorithms, though provided valuable algorithms, did not focus on service reliability benefits from activating residential DR potentials.

According to the above discussion, the literature lacks a model that coordinates residential consumers' responses for the purpose of network reliability improvement. To address this gap, this paper introduces a centralized model designed to adjust consumers' load profile in response to unexpected events. The primary objective of this model is to minimize the costs of load curtailment that an unforeseen event can impose on the distribution company. The proposed scheme operates under the assumption that the Distribution System Operator (DSO) and customers have already signed a contract authorizing the DSO to modify the operation of customers' responsive appliances, as long as their preferences and comfort are not compromised. In the model, customers who signed the contract provide the DSO with information regarding their responsive loads and preferences. Using the information provided by customers, the DSO considers distribution network constraints and schedules responsive loads in a way that satisfies violated network operating limits. Of note, load curtailment is the measure of last resort in the proposed model. The model is mathematically formulated in the form of Mixed Integer Linear Programming (MILP) and guarantees obtaining a global optimum solution. In summary, the main contributions of the paper are listed as follows:

1. This paper introduces the model that coordinates residential consumers' responses for the purpose of network reliability improvement by considering responsive appliances and Plugged-in Hybrid Electric Vehicles (PHEVs);
2. To coordinate residential DR potentials, a centralized framework is utilized to adjust consumers' load profiles to minimize load curtailment costs following unexpected events. The model ensures that consumers' preferences and comfort are not compromised;
3. The model is mathematically formulated in the form of MILP that can be efficiently solved using off-the-shelf commercial solvers and the capability of the model is examined through its implementation on a real-world network with real information.

The rest of the paper is organized as follows. The system model is introduced in Section 2. The mathematical formulation of the model is presented in Section 3 where DR scheme, distribution network, and responsive load models are proposed. Case studies, simulation results, and discussion are provided in Section 4. Finally, Section 5 concludes the paper.

2. System model and problem description

In the considered smart distribution system, DSO and

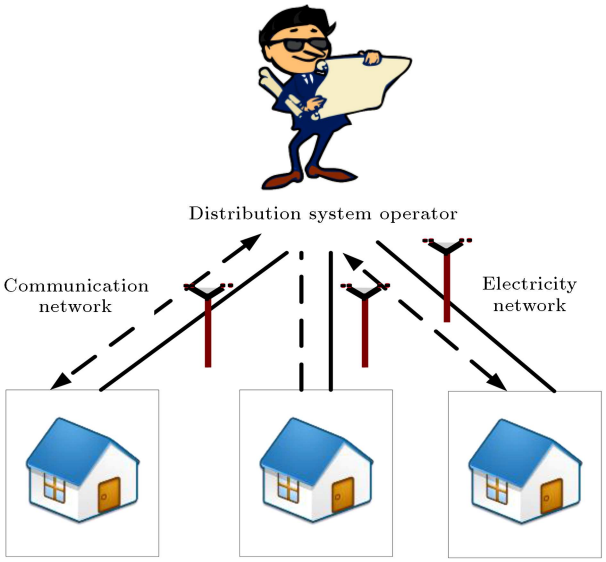

Figure 1. A typical smart distribution system.

multiple residential customers are the agents. As illustrated in Figure 1, a two-way communication infrastructure enables signal exchanging between DSO and active customers. It is assumed that the DSO signed a contract with some customers (called responsive or active customers) to directly control their responsive appliances under customers' constraints. Customers who signed the contract provide the DSO with data about their responsive loads as well as constraints related to their preferences and comforts. By receiving these data, DSO considers the operational constraints of distribution network, as well. DSO optimizes the utilization of responsive customers for minimizing imposed costs in emergency situations.

The objective is to minimize the total interruption cost imposed on the DSO following an unexpected event. DSO commits the responsive appliances of active consumers and plans the charging and discharging cycles of customer PHEVs in a way that meets the objective. The responsive appliances of each active customer include washing machine, dishwasher, and clothes dryer. Furthermore, the charging and discharging cycles of customer PHEVs are controlled in the proposed model. Once the optimization problem is solved and the optimum operating periods with the amount of load shedding are determined, the DSO sends control signals to customers' smart meters through communication infrastructures. The smart meters embedded in customer houses control individual responsive appliances based on the received signals. Figure 2 shows a typical home area network. As can be seen, the Zigbee-based network shown in the figure enables the smart meter to switch on/off all responsive appliances such as washing machine and dish washer and to control the charging and discharging cycles of PHEVs.

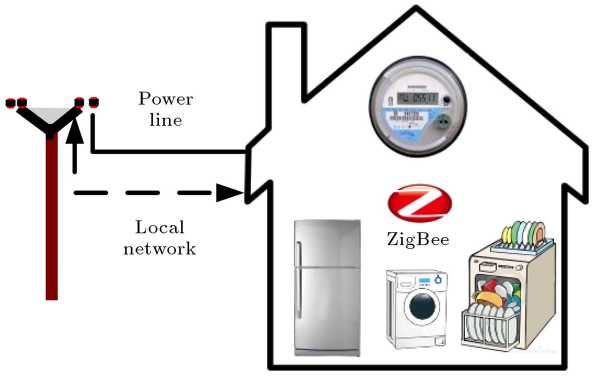

Figure 2. A typical smart home equipped with a home area network.

3. Mathematical formulation

As described in Section 2, DSO intends to minimize the imposed costs due to unexpected events. In this section, the mathematical formulation of the DSO optimization problem is presented. The proposed optimization model is solved for each probable contingency and each day under study in order to optimally utilize residential DR resources to minimize the interruption costs following the occurrence of each contingency. In Section 3.5, the technique for assessing network reliability and acquiring corresponding reliability indices is presented. The input of the model contains two sets of data. The first set includes the data associated with customers' responsive appliances and their comfort limits. The data of the underlying distribution network and its operational constraints build the second data set. The model's output, which takes into account various constraints, includes the optimal load that is curtailed from both passive and active customer demands, as well as the operating status of responsive appliances, charging/discharging rates, and the associated periods of PHEVs.

3.1. Objective

By executing the residential DR program, DSO aims to minimize the total costs imposed due to unexpected events, as expressed in Eq. (1). The imposed cost is composed of two general terms. The first term is the sum of interruption costs due to load curtailment. Furthermore, the sum of bills that should be paid for purchasing electricity from the wholesale market, the incomes from selling energy to customers, and the money paid to the responsive customers for utilizing their responsive loads should be accounted as the second term of DSO costs. Of note, when the network experiences contingency, the first term dominates the second one because of the high Value Of Lost Load (VOLL); hence, the second term is not considered in the objective function. The following equation formulates the objective function, where $PC_{NR}^{b,t}$ and $PC_{R}^{n,t}$ are curtailed loads from non-responsive and

responsive loads, respectively. To curtail each unit of either responsive or non-responsive loads, a significant penalty (i.e., VOLL) should be paid to the consumers:

$$TIC = \sum_{b\in B}\sum_{t\in T}\left(PC_{NR}^{b,t} + \sum_{n\in NB} PC_{R}^{n,t}\right) \times VOLL_b. \quad (1)$$

The objective is to minimize the total cost by considering the following constraints. It should be noted that the presented models in Sections 3.2 and 3.3 will be linked to the objective function through the constraints presented in Section 3.4.

3.2. Responsive appliances

To ensure the complete operation of responsive appliances and the convenience of customers, it is important to take into account constraints that may affect their operation. In this paper, instead of assuming the uniform power consumption for appliances, the real consumption pattern based on Energy Consumption Profile (ECP) of appliances is taken into account. A sample ECP for a washing machine is depicted in Figure 3 [21]. For each appliance, the required energy for complete operation should be provided. The total required energy of each appliance is equal to the surface under its ECP. The set of Eq. (2) ensures that this requirement is satisfied. These expression sets also guarantee the continuous operation of each appliance. To put it differently, every appliance consumes the power it requires at each time interval following its associated ECP once it has been started up.

$$P_a^{n,t} = \sum_{i=1}^{k_a} z_a^{n,t-k_a+i}.p_a^{k_a-i+1},$$

$$\forall n \in N,\ \forall a \in A,\ \forall t \in T. \quad (2)$$

In Eq. (2), $z_a^{n,t}$ is a binary variable denoting the startup status of appliance a for customer n at time step t. $z_a^{n,t}$ is equal to 1 if the appliance is initiated at the associated time step; otherwise, it is equal to 0. The nominal power of appliance a at time step k in the ECP is obtained from the related ECP, which is denoted by p_a^k. For the washing machine, p_a^k at the second time step is equal to 2000 W. Moreover, it should be noticed that k_a is the number of required time steps for complete operation of appliance a, which is equal to 8 for washing machine. The given equation indicates that starting an appliance at time step t aligns the appliance's consumption profile with its associated ECP between the time intervals of $[t, t + ka - 1]$. For instance, let's assume that the value of z is 1 for a washing machine at $t = 12$. At $t = 12$, when i is equal to 8 in Eq. (2), $z = 1$ (it should be noted that $k_a = 8$); hence, $P_a^{n,t}$ at $t = 12$ is equal to p_a^1. It is implied that the consumption power of washing machine at $t = 12$ is equal to the power of the first interval of ECP. In addition, at $t = 15$ (i.e., the fourth interval after startup), z is equal to 1 for $i = 5$. Hence, $P_a^{n,t}$ at $t = 15$ is equal to p_a^4.

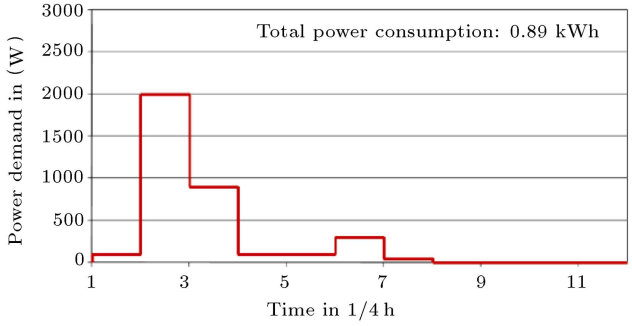

Figure 3. ECP of washing machine [21].

Each customer who participates in the DR program delivers allowed starting and ending times of its responsive appliances. Responsive appliances must operate during this time interval, i.e., during interval $[\alpha_a^n, \beta_a^n]$. The following set of constraints guarantees this rule. One constraint specifies that appliances cannot be started during the undesired intervals of customers. In other words, each appliance a for customer n can only be started between α_a^n and $\beta_a^n - k_a + 1$. $\beta_a^n - k_a + 1$ in Eq. (3) ensures that an appliance has adequate time after being started up to consistently consume the necessary energy required to complete its task. Furthermore, Eq. (4) ensures that each appliance can operate only once on a typical day. The use of responsive appliances by customers on a typical day is determined based on statistical data [21]. It should be noted that these hard constraints guarantee compliance to customer comfort.

$$z_a^{n,t} = 0, \quad \forall n \in N, \quad \forall a \in A,$$

$$\forall t \in T - [\alpha_a^n, \beta_a^n - k_a + 1], \quad (3)$$

$$\sum_{t\in T} z_a^{n,t} = 1, \quad \forall n \in N, \quad \forall a \in A. \quad (4)$$

Finally, the consumed reactive power of responsive appliances is calculated in Eq. (5):

$$P_a^{n,t} = Q_a^{n,t} \times PQR_R^{n,t}, \quad \forall n \in N, \quad \forall a \in A, \quad \forall t \in T. \quad (5)$$

3.3. Plugged-in Hybrid Electric Vehicle (PHEVs)

In various countries, there has been a recent increase in the penetration level of PHEVs. In addition, DR strategies and incentive mechanism have been introduced to encourage the owners to participate in DR program. They utilize rechargeable batteries that can be charged by connecting their plug to network. PHEVs are usually connected to grid upon arriving at home. This period of time, however, usually coincides with the peak interval of residential loads;

therefore, controlling the charging time of PHEVs by the DR program not only fulfills the objective but also overcomes their disadvantages.

A number of constraints should be satisfied first before modeling PHEVs. In this paper, charging/discharging cycles of the PHEVs are controlled to fulfill the objective. It is worth noting that because of the positive impact of utilizing the discharge power of PHEVs through Vehicle to Grid (V2G) infrastructure, controlling both charging and discharging power of PHEVs is considered in this paper [22,23]. This study presents a model for utilizing PHEV batteries based on the travel patterns of their owners. Since the PHEV battery cannot be charged and discharged simultaneously, the study includes Constraint (6). It is important to note that Constraint (6) is only considered for the interval during which the vehicle is at home. During the out-of-home period, both $x^{n,t}_{ch\_p}$ and $x^{n,t}_{dch\_p}$ must be equal to zero since customers cannot charge or discharge PHEVs at home:

$$x^{n,t}_{ch\_p} + x^{n,t}_{dch\_p} \leq 1,$$
$$\forall\, n \in NP, \quad \forall\, t \in [\alpha^n_{PHEV},\, \beta^n_{PHEV}]\,. \tag{6}$$

The arrival and departure times of PHEVs are important factors and are denoted by α^n_{PHEV} and β^n_{PHEV}, respectively. The arrival and departure times of vehicles to/from home are generated based on the historical data presented by NHTS [24]. Numerous historical data sets of PHEVs' arrival and departure have been taken from NHTS. Then, these datasets are classified based on the attained probability distribution functions. By using Monte-Carlo approach, different arrival/departure times are assigned to each customer for each day under study. During the journey interval when a PHEV is away from home, its battery cannot be charged or discharged. Therefore, it is necessary to satisfy the set of Eqs. (7) and (8):

$$x^{n,t}_{ch\_p} = 0,$$
$$\forall\, n \in NP, \quad \forall t \in T - [\alpha^n_{PHEV},\, \beta^n_{PHEV}]\,, \tag{7}$$
$$x^{n,t}_{dch\_p} = 0,$$
$$\forall n \in NP, \quad \forall t \in T - [\alpha^n_{PHEV}, \beta^n_{PHEV}]\,. \tag{8}$$

The charging and discharging rates of the PHEV battery should be mounted between minimum and maximum allowable ranges which is preserved through the set of Constraints (9) and (10). The product of binary variables $x^{n,t}_{ch\_p}$ and $x^{n,t}_{dch\_p}$ to the sides of Constraints (9) and (10) forces the charging and discharging energies of battery into zero when charge or discharge decisions are not taken:

$$\underline{E}^{\,n}_{ch\_p}.\, x^{n,t}_{ch\_p} \leq E^{n,t}_{ch\_p} \leq \overline{E}^{n}_{ch\_p}.x^{n,t}_{ch\_p},$$
$$\forall n \in NP, \quad \forall t \in T, \tag{9}$$
$$\underline{E}^{\,n}_{dch\_p}.\, x^{n,t}_{dch\_p} \leq E^{n,t}_{dch\_p} \leq \overline{E}^{n}_{dch\_p}.x^{n,t}_{dch\_p},$$
$$\forall n \in NP, \quad \forall t \in T. \tag{10}$$

The important factor of the PHEV batteries is their State of Charge (SoC) at each time step. Battery SoC of the PHEV is determined via Eqs. (11) and (12), where E^n_{0p} is the SoC of battery at the time of arrival, also called initial SoC:

$$SoC^{n,t}_p = E^n_{0p} + \left(\eta^n_{ch\_p}.E^{n,t}_{ch\_p} - \frac{1}{\eta^n_{dch\_p}}.E^{n,t}_{dch\_p}\right),$$
$$\forall n \in NP, \quad \forall t = \alpha^{\,n}_{PHEV}, \tag{11}$$
$$SoC^{n,t}_p = SoC^{n,t-1}_p + \left(\eta^n_{ch\_p}.E^{n,t}_{ch\_p} - \frac{1}{\eta^n_{dch\_p}}.E^{n,t}_{dch\_p}\right),$$
$$\forall n \in NP, \quad \forall t \in (\alpha^n_{PHEV}, \beta^n_{PHEV}]. \tag{12}$$

The SoC of all PHEVs' batteries at time interval t should be positive, but lower than their maximum capacity. These conditions are stated in the set of Constraint (13). The constraint of positive SoC in Constraint (13) can be stated in the form of Constraint (14), which implies that the discharging energy at each time interval cannot be more than the SoC at the previous time step.

$$0 \leq SoC^{n,t}_p \leq \bar{E}^n_p,$$
$$\forall n \in NP, \quad \forall t \in T, \tag{13}$$
$$\frac{1}{\eta^n_{dch\_p}}.E^{n,t}_{dch\_p} \leq SoC^{n,t-1}_p,$$
$$\forall n \in NP, \quad \forall t \in T. \tag{14}$$

Before leaving home, the SoC of the PHEV's battery should be sufficient for the next journey. It is worthwhile to mention that PHEVs can decrease the curtailed load by deferring their charging; however, if a PHEV's battery is not charged until the required level, the interruption cost is paid to the PHEV owner. It should be noted that Constraints (7), (8), and (15) guarantee customer comfort in the case of using their PHEVs:

$$SoC^{n,t}_p \geq E^n_p,$$
$$\forall\, n \in NP, \forall t = \beta^n_{PHEV}. \tag{15}$$

The average amounts of charging/discharging powers are calculated and and considered at each time

interval based on the charging/discharging energies. The relations between average charging/discharging powers and charging/discharging energies are described in Eqs. (16) and (17), respectively. It should be noted that the duration of each time interval (Δt) is equal to 0.25 hours. Based on the characteristics of battery charger, the amounts of consumed reactive powers during charging and discharging periods are obtained by Eqs. (18) and (19):

$$E^{n,t}_{ch\_p} = P^{n,t}_{ch\_p} \times \Delta t, \quad \forall n \in NP, \quad \forall t \in T, \tag{16}$$

$$E^{n,t}_{dch\_p} = P^{n,t}_{dch\_p} \times \Delta t, \quad \forall n \in NP, \quad \forall t \in T, \tag{17}$$

$$P^{n,t}_{ch\_p} = Q^{n,t}_{ch\_p} \times PQR^{n,t}_{PHEV}, \quad \forall n \in NP, \quad \forall t \in T, \tag{18}$$

$$P^{n,t}_{dch\_p} = Q^{n,t}_{dch\_p} \times PQR^{n,t}_{PHEV}, \quad \forall n \in NP, \quad \forall t \in T. \tag{19}$$

3.4. Distribution network constraints

Households are hosted by the distribution network which makes it necessary to consider power flow and network operational constraints. If the effect of distribution network is ignored and the balance between supply and demand is considered, the output of the problem may be unrealistic and lead to violation of network operational limits. As a result, the constraints imposed by the distribution network are included in the proposed model.

The two following sets of constraints ensure balance between the bus-level active and reactive powers:

$$P^{b,t}_{NR} + \sum_{n \in NB} \left(P^{n,t}_{Fixed} + P^{n,t}_{ch\_p} - P^{n,t}_{dch\_p} + \sum_{a \in A} P^{n,t}_{a} \right) + \sum_{b' \in B} PF^{t}_{b,b'} = PC^{b,t}_{NR} + \sum_{n \in NB} PC^{n,t}_{R}, \quad \forall b \in B, \quad \forall t \in T, \tag{20}$$

$$Q^{b,t}_{NR} + \sum_{n \in NB} \left(Q^{n,t}_{Fixed} + Q^{n,t}_{ch\_p} - Q^{n,t}_{dch\_p} + \sum_{a \in A} Q^{n,t}_{a} \right) + \sum_{b' \in B} QF^{t}_{b,b'} = QC^{b,t}_{NR} + \sum_{n \in NB} QC^{n,t}_{R}, \quad \forall b \in B, \quad \forall t \in T. \tag{21}$$

In order to calculate active and reactive power flows through lines, the following linear equations are used:

$$PF^{t}_{b,b'} = L^{t}_{b,b'} \times \left[-\frac{1}{2} G_{b,b'} (V^{2}_{b,t} - V^{2}_{b',t}) + B_{b,b'} (\delta_{b,t} - \delta_{b',t}) \right], \quad \forall (b,b') \in L, \quad \forall t \in T. \tag{22}$$

$$QF^{t}_{b,b'} = L^{t}_{b,b'} \times \left[\frac{1}{2} B_{b,b'} (V^{2}_{b,t} - V^{2}_{b',t}) + G_{b,b'} (\delta_{b,t} - \delta_{b',t}) \right], \quad \forall (b,b') \in L, \forall t \in T. \tag{23}$$

For deriving the above equations, active and reactive losses of the distribution network are neglected. The resulting equations are linear with respect to the square of voltage amplitudes. For detailed information about solving the above two equations, inspired readers are referred to [25].

Amplitude of bus voltages should be mounted between lower and upper limits and is adhered by Eq. (24). Furthermore, the angle of bus voltages should satisfy Constraint (25). It should be explained that Eqs. (22) and (23) are linear with respect to the square of voltage amplitude. Therefore, in order to preserve the linearity of the model, in Constraint (24), the square of voltage magnitude is considered to be equal to the square of allowable lower and upper bounds.

$$\underline{V}^{2} \leq V^{2}_{b,t} \leq \bar{V}^{2}, \quad \forall b \in B, \quad \forall t \in T, \tag{24}$$

$$-\pi \leq \delta_{b,t} \leq \pi, \quad \forall b \in B, \quad \forall t \in T. \tag{25}$$

Line active power flow limits are taken into account as follows:

$$-PF^{t}_{sys} \times \bar{S}_{b,b'} \leq PF^{t}_{b,b'} \leq PF^{t}_{sys} \times \bar{S}_{b,b'}, \quad \forall (b,b') \in L, \quad \forall t \in T. \tag{26}$$

To ensure that the power factor remains constant by shedding the load, the two following sets of constraints are incorporated:

$$PC^{b,t}_{NR} = QC^{b,t}_{NR} \times PQR^{b,t}_{NR}, \quad \forall b \in B, \quad \forall t \in T, \tag{27}$$

$$PC^{n,t}_{R} = QC^{n,t}_{R} \times PQR^{n,t}_{R}, \quad \forall n \in N, \forall t \in T. \tag{28}$$

The minimum and maximum capabilities of load curtailments associated with passive and active customers are declared as follows:

$$0 \leq PC^{b,t}_{NR} \leq P^{b,t}_{NR}, \quad \forall b \in B, \quad \forall t \in T. \tag{29}$$

$$0 \leq PC^{n,t}_{R} \leq P^{n,t}_{fixed} + P^{n,t}_{ch\_p} + \sum_{a \in A} P^{n,t}_{a}, \quad \forall n \in N, \quad \forall t \in T. \tag{30}$$

3.5. Reliability evaluation for the network

As clarified in the previous sections, the proposed model is considered for each contingency. In other words, following the occurrence of each contingency, the proposed model minimizes the costs of interruptions through optimal utilization of residential DR resources. In this section, the method of assessing the distribution network reliability and calculating the associated reliability indices is presented and the associated flowchart is depicted in Figure 4. In order to perform reliability analysis, three main steps are taken into account:

1. *Gathering probable scenarios*: In this paper, we use the state enumeration technique to identify all $N-1$ contingencies that may occur due to active failures in the network branches. Note that the probability of two simultaneous outages occurring is too low and the $N-1$ criterion is very commonly used in distribution networks. By considering the occurrence of active failure in the branches, protective switches are opened to stop feeding power to the fault location. Then, the switching actions are done to energize the interrupted customers considerably. It is assumed that the switching action of circuit breakers is managed through automatic remote control; however, isolating faulty branches takes long, equal to switching time (1 hour in this paper). Following the occurrence of a contingency, the status of network branches (i.e., in service or out of service) at each time interval (i.e., during switching and repair times) is determined and is considered in the proposed model by defining $L^t_{b,b'}$. If the branches between two nodes b and b' be out of service, then $L^t_{b,b'}$ in Eqs. (22) and (23) is set to 0 to demonstrate the network topology after fault occurrence;
2. *Contingency analysis*: In this step, the proposed optimization problem (Relations (1)–(30)) is solved for each contingency and the outcome for every single case of contingency is determined. In other words, once the network experiences a fault, by determining a new network topology (as described in Step 1), the optimal amount of curtailed load at each load point as well as the optimal utilization of responsive resources are obtained in order to prevent network violation. In the optimization problem, the effect of DR as the main contribution is investigated. In other words, in emergency situations, the DR capability of responsive loads is utilized first. Then, if required, the last resort is load curtailment. Therefore, using the DR potential of responsive loads helps postpone electricity usage in emergency conditions, resulting in further reduction of curtailed load. In summary, the utilization of DR for enhancing network reliability based on the proposed model is addressed in this step;
3. *Calculating reliability indices*: The service reliability indices evaluated in this paper include Expected Energy Not Served (EENS), System Average Interruption Frequency Index (SAIFI), System Average Interruption Duration Index (SAIDI), and Expected Interruption Cost (EIC). The mathematical formula of the above-mentioned indices is given through Eqs. (31)–(34) in the following [26]:

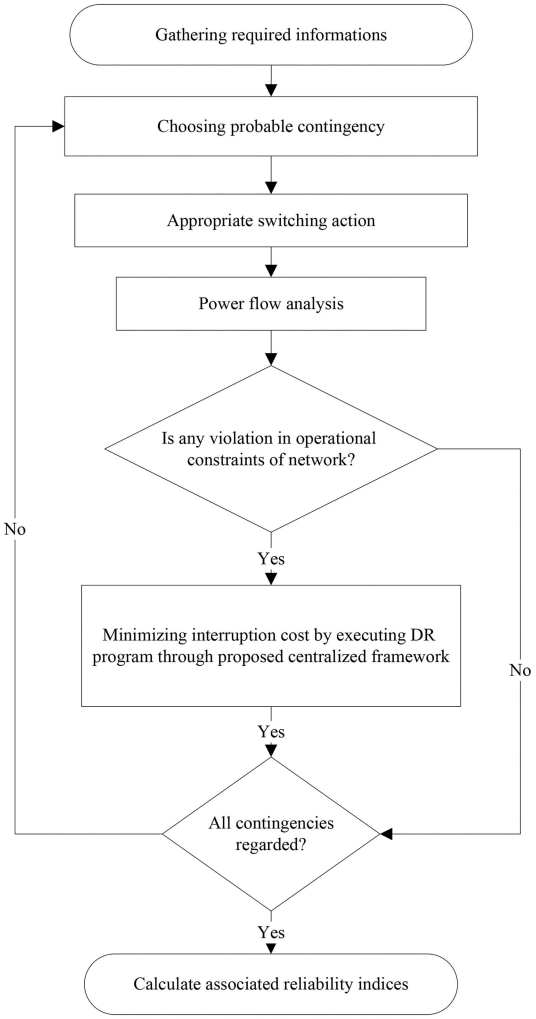

Figure 4. Procedure of reliability analysis considering DR program.

$$EENS = \sum_{c \in C} \sum_{b \in B} \sum_{t \in T} \lambda_c \times \left(PC_{NR}^{b,t,c} + \sum_{n \in NB} PC_R^{n,t,c} \right) \Delta t, \quad (31)$$

$$SAIFI = \frac{\sum_{b \in B} \lambda_b . NC_b}{\sum_{b \in B} NC_b}, \quad (32)$$

$$SAIDI = \frac{\sum_{b \in B} U_b.NC_b}{\sum_{b \in B} NC_b}, \tag{33}$$

$$EIC = \sum_{c \in C} P_c.TIC_c, \tag{34}$$

where λ_c, P_c, and TIC_c are the failure rate, probability, and total interruption cost of contingency c, respectively. In addition, NC_b, λ_b, and U_b represent the number of customers, equivalent failure rate, and equivalent repair time at bus b, respectively. The above indices are formulated for one typical day. It should be explained that the information about the time of failure or its associated probability is not available. On the other hand, because of the varying loads of the network and varying flexibility of responsive loads during 24 hours of a day, the effect of the time of fault occurrence should be considered in the model. To calculate the reliability indices, the occurrence of contingencies at different hours of a day is considered; finally, the average value of indices over 24 hours is considered.

In order to calculate the reliability indices over the year, the proposed model is solved for 8 days. In this regard, for each season, 2 days are considered, one for weekdays and another for weekends. These 8 days are representative of all 365 days in the year and the results obtained for these 8 days are extended to obtain the indices over the year. For each of the 8 mentioned days, the indices are calculated using Eqs. (31)–(34). To calculate the values of indices for each day, they are averaged over 24 hours by considering the occurrence of contingencies at different hours of a day. After obtaining indices for 8 studied days, to compute the indices over the year, they are multiplied by the number of days that they have been representative for them. For example, the indices obtained for a weekday of the summer are multiplied by 68. Finally, the weighted indices of 8 studied days are summed up.

4. Numerical results

In this section, the proposed centralized DR scheme is applied to a finnish distribution network with total 200 customers. The distribution network under study is illustrated in Figure 5. As depicted earlier, this network feeds 61 load points through 2 radial feeders with a normally open tie line between them. The input data of the model including load and customer data, reliability parameter, and technical data of the network are presented in the Appendix.

Two major case studies, namely base case and DR enabled case, are conducted and the associated results are compared. In the base case, all of the customers are passive and their load profiles correspond

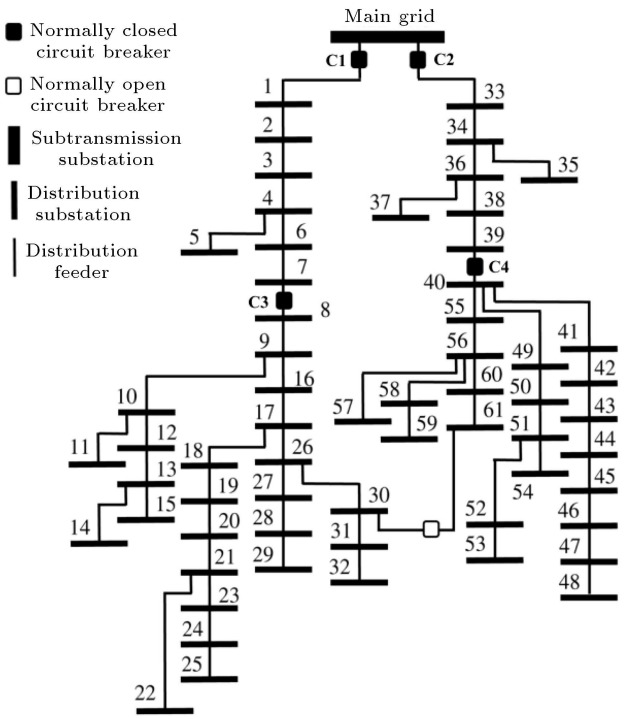

Figure 5. Single line diagram of finnish distribution network under study.

to their usual consumption pattern, whereas in the DR enabled case, a portion of customers at each bus are responsive and their responsive loads can be scheduled by DSO in order to fulfill the objective. In this case, responsive customers receive an incentive to change their load profile based on the signals received from DSO in order to increase the reliability of distribution systems. In the following, the performance of the proposed model during a few likely contingencies is evaluated. In this regard, for evaluating the impact of DR on the reliability indices of customers, it is assumed that all of 200 customers actively participate in DR program. Then, the system-oriented reliability indices are reported. For the last part of this study, a sensitivity analysis of the penetration level of active customers is performed and the effect of customers' position in the network on the system reliability indices is evaluated. It is notable that the proposed MILP model is solved using CPLEX 12.0 solver [27].

4.1. Evaluating four likely contingencies

In this section, the proposed model's effectiveness is evaluated by simulating a number of likely contingencies and observing the resulting outcomes. In each case, some important parameters are compared with those in the base case. It should be mentioned that four contingencies illustrate faults that occur in different parts of the network and at different times of a typical day.

Contingency 1: In this case, a fault takes place

Table 1. Comparison of service reliability indices in Contingency 1.

Index	Base case	DR enabled
Number of affected customers	68	68
Average interruption duration (h)	2.8182	2.8182
ENS (kWh)	288.9	198.7
Interruption cost (€)	7615.6	5232.8

Table 2. Comparison of service reliability indices in Contingency 2.

Index	Base case	DR enabled
Number of affected customers	88	88
Average interruption duration (h)	1.50	1.05
ENS (kWh)	215.7	78.4
Interruption cost (€)	4044.4	1634.2

in sections 40–41 at 18:00. Through this fault, the upstream circuit breaker isolates load points 40 to 61. After the switching time (assumed to be 1 hour here), by isolating the faulty section and closing the upstream circuit breaker, load points 40 and 49–61 are restored, while load points 41–48 remain isolated until the end of repair time (assumed to be 6 hours here). During the switching time, the operation of responsive appliances of active customers situated at load points 40 and 49–61 can be delayed to reduce the amount of energy not served and the associated interruption costs. On the other hand, DR cannot be effective for the number of affected customers and interruption duration of load points 41–48 because the allowable deferring time of responsive appliances is shorter than the repair time. Table 1 compares the reliability indices of the mentioned contingency for the two case studies. As can be concluded, the energy not served and the associated interruption costs are reduced by 30.8% and 31.1%, respectively, after enabling DR. The number of affected customers and average interruption duration remain unchanged;

Contingency 2: A fault occurs on branch 8–9 at 20:00 and causes the upstream beaker to operate. Load points 8–32 are isolated after the circuit breaker operation. During the switching time, the mentioned load points remain interrupted. By isolating the faulty section and closing the tie switch, the right-side feeder must supply customers situated at load points 9–32. In the base case scenario where no responsive customers are present, due to limited tie line capacity and voltage amplitude limits of buses, only a few isolated customers can be energized during the repair period. By enabling residential DR potentials, it is possible to solve the overload problem and feed more customers during repair time. Furthermore, during switching time, the amount of load curtailed is reduced in this case. Comparison of the reliability indices for this contingency is given in Table 2. As is shown, the average interruption duration, energy not served, and the associated damage costs are reduced considerably, while the number of affected customers is the same in both case studies. The energy not served and damage costs indices are reduced by 63.7% and 59.6%, respectively;

Contingency 3: In this case, section 1–2 experiences a fault at 14:00. The upstream circuit breaker is opened and load points 1–32 are isolated. Through appropriate switching actions, customers connected to load points 8–32 are transferred to the neighboring feeder. Following the fault, in both the base and DR-enabled cases, customers connected to load points 1–7 are interrupted during the switching time. In order to restore the customers hosted by load points 8–32, the circuit breaker laid in section 7–8 is opened and the tie switch is closed. In doing so, a portion of the customers are energized through the neighboring feeder and merely experience a momentary interruption. It is worth mentioning that not all of customers are restored because of overload and low voltage condition in the neighboring feeder. In the DR enabled case, it is possible to energize more customers by the switching action since the overload condition is partly mitigated through load management. The reliability indices of the base case and the DR-enabled case during the contingency are compared, as shown in Table 3. As can be seen, the number of affected customers is significantly reduced in the DR-enabled case. Also, other reliability indices are enhanced in the DR-enabled case. In this case, energy not served and interruption costs are enhanced by 47.8% and 41.0%, respectively.

Table 3. Comparison of service reliability indices in Contingency 3.

Index	Base case	DR enabled
Number of affected customers	62	21
Average interruption duration (h)	1.2	1.00
ENS (kWh)	125.0	65.2
Interruption cost (€)	2579.6	1521.8

Table 4. Comparison of service reliability indices in Contingency 4.

Index	Base case	DR enabled
Number of affected customers	68	68
Average interruption duration (h)	1.00	1.00
ENS (kWh)	77.0	49.1
Interruption cost (€)	1881.9	1201.9

As mentioned earlier, it is assumed that the circuit breakers C1–C4 and the tie line switch can be controlled remotely in coordination with each other. Furthermore, the branch isolators (like isolators of branches between nodes 8 and 9) are manually controlled and changing their position takes a long time equal to the switching time (1 hour in this paper). In Contingency 3, when branch 1–2 experiences a fault, the circuit breaker C1 is opened after which the circuit breaker C3 is opened. In this condition, the faulted section is isolated from the network under C3 and load points 8–32 are energized by closing the tie-line switch. These switching actions are assumed and handled through automatic remote control infrastructure; hence, load points 8–32 experience momentary interruption. It should be explained that in Contingency 2, when branch 8–9 experiences a fault, the circuit breaker C3 is opened to stop feeding the fault location. The crew team performs the isolation of branch 8–9, which takes a long time equivalent to the switching time of 1 hour. After the isolation is complete, the tie-line switch is closed to energize load points 9–32. The tie-line switch cannot be closed before isolating the fault location. Hence, load points 9–32 remain unenergized for 1 hour. In general, if the fault occurs between the circuit breakers C1 and C3 or between circuit breakers C2 and C4, the load points under C3 and C4 experience momentary interruption and can be rapidly transferred to a neighboring feeder through automatic switching operation. In this case, the application of the proposed DR framework can feed more customers after remote switching, leading to SAIFI improvement;

Contingency 4: An unexpected event occurs in section 60–61 at 17:00. Following this fault, the upstream circuit breaker operates and isolates load points 40–61. The customers fed from these load points experience interruption during the switching time. By opening the faulty section and closing the tie line, all customers are restored. During the repair time, load points 40–60 are fed through the right-side feeder and load point 61 is fed by the neighboring feeder. In both cases, namely base and DR-enabled cases, all of the load points are energized after switching time due to no overload issue. However, in the DR-enabled case, by utilizing the flexibility of responsive loads, the amount of load shedding and its associated costs are reduced during switching time. Table 4 compares the reliability indices for the two study cases following the occurrence of the mentioned contingency. The number of affected customers and the duration of the interruption remain the same in both cases. This is because during the switching time, all customers fed through load points 40–61 are isolated and at least their non-responsive loads are curtailed. The amount of energy not served and the associated damage costs are reduced by 36.1% in case of utilizing DR potentials of residential customers.

4.2. General results

In the previous sub-sections, the impacts of activating residential DR on the system reliability during four individual contingencies were demonstrated. This section evaluates the impact of executing the proposed DR program on the overall reliability of the distribution system. To assess the distribution network reliability, as explained in Section 3.5, all credible contingencies during the days under study are considered and the obtained results are combined to investigate the system-oriented reliability indices during the year. Table 5 compares the system-oriented reliability indices in both base case and DR-enabled case. The presented results

Table 5. System-oriented reliability indices.

Index	SAIFI (occ/cust.yr)	SAIDI (h/cust.yr)	EENS (kWh)	EIC (€)
Base case	0.0708	0.1464	57.3548	1319.6
DR enabled	0.0631	0.1264	39.2241	942.8
Improvement (%)	10.88	13.66	31.61	28.55

Table 6. Indices of invoked DR potentials in the DR-enabled case.

EPE (kWh)	EIF_a (occ/appl.yr)	EIF_c (occ/cust.yr)	EID_a (h/occ.app)	EID_c (h/occ.cust)
19.0421	0.2589	0.3793	0.5687	1.7060

Table 7. System oriented reliability indices for different penetration levels of active customers.

Penetration level of active customers (%)	SAIFI (occ/cust.yr)	SAIDI (h/cust.yr)	EENS (kWh)	EIC (€)
0 (Base case)	0.0708	0.1464	57.3548	1319.6
25	0.0670	0.1349	49.0024	1152.0
50	0.0660	0.1332	46.1124	1101.1
75	0.0640	0.1279	41.8240	995.9
100	0.0631	0.1264	39.2241	942.8

show the significant impacts of the proposed method on the reliability of the distribution network. Of note, this level of improvement is achieved due to the flexibility of three responsive appliances and PHEVs of customers, without sacrificing their preferences. Responsive appliances of each customer include washing machine, dishwasher, and clothes dryer, while the charging/discharging cycles of customers' PHEVs are controlled. The energy consumption of the mentioned responsive appliances is about 30% of the total energy consumption of each customer. The obtained results in this section demonstrate that the flexibility of residential responsive loads can reduce the EIC by around 28%. In addition, execution of the DR program improves reliability indices, as well. Relevant research findings confirm the significant impact of DR on the reliability of the network.

As mentioned before, the network reliability is improved by deferring responsive appliances of active customers. In an ideal network, deferring loads is not a desirable action. Table 6 presents invoked DR potentials in the DR-enabled case. In this table, "EPE" represents the expected postponed energy of responsive customers. "EIF_a" and "EIF_c" introduce expected interruption frequency of responsive appliances and customers, respectively. In addition, "EID_a" and "EID_c" represent the expected interruption duration of responsive appliances and customers, respectively. As can be seen, this significant improvement of system reliability is obtained by merely deferring responsive loads (including PHEVs) about 30 minutes in 0.26 times a year. To ensure this improvement, responsive customers are deferred by less than 2 hours in 0.38 times a year. On the other hand, for achieving this level of system reliability improvement, we need to defer responsive loads only for a few minutes a year.

4.3. Sensitivity analysis

The penetration level of active customers in the network is an important and effective factor in DR capability and consequent reliability improvement. In the previous section, the studies were conducted by assuming 100% penetration level of active customers in the distribution network. This means that in the DR-enabled case, all customers actively participate in DR program. It is an unreal assumption in a real-world distribution network, because there are a limited number of customers who may sign a contract with DSO. For this reason, in this section, the effect of the penetration level of active customers on the system reliability indices and invoked DR potential indices is evaluated. It should be noted that the penetration level of responsive customers at each bus of the network is assumed the same. System reliability indices of the distribution network for different penetration levels of customers are shown in Table 7. It can be seen that the reliability indices are improved as the penetration level of active customers increases.

Invoked DR potential indices at different penetration levels of active customers are compared in Table 8. It can be seen that by increasing the penetration level of active customers, the frequency and duration of load deferring are reduced.

4.4. Position of active customers analysis

One of the challenges of DSO in designing a DR program is the fact of fairness in contracts. In other words, DSO is interested to make a contract with and pay to

Table 8. Indices of DR potential invocation for different penetration levels of active customers.

Penetration level (%)	EPE (kWh)	EIF_a (oc/app.yr)	EIF_c (oc/cust.yr)	EID_a (h/oc.app)	EID_c (h/oc.cu)
25	10.1979	0.2850	0.4026	0.5997	1.7991
50	12.4983	0.2756	0.3964	0.5841	1.7424
75	17.1039	0.2722	0.3930	0.5749	1.7246
100	19.0421	0.2589	0.3793	0.5687	1.7060

Table 9. Percentage of reliability indices improvement for customers hosted in different places of network.

Position of customers	SAIFI improv. (%)	SAIDI improv. (%)	EENS improv. (%)	EIC improv. (%)
Main feeders	12.39	17.24	31.87	31.11
Laterals	9.99	12.54	29.12	26.94
Upper half	10.22	13.22	28.92	27.35
Lower half	10.76	13.41	29.82	27.92

customers who are able to improve system reliability effectively. On the other hand, customers supplied with a high level of reliability should pay more to the DSO. In this section, two different studies are conducted. In the first study, the effect of executing a designated DR program on the reliability indices of customers in different parts of the network is evaluated. The second study focuses on the effectiveness of enabling DR potentials of customers connected in different parts of the network.

In the first study, it is assumed that all of the customers actively change their responsive loads. The improvement of reliability indices of the customers hosted in the main feeder, laterals, lower half, and upper half of the network is presented in Table 9. As can be seen, customers who are fed through the main feeders experience significantly greater improvements in their reliability indices compared to those fed through laterals. In addition, by comparing the customers who are hosted in the upper half and lower half of the network, it can be seen that the improvement of reliability indices in the lower half of the network is more significant.

In the second study, the DR potential of customers in different parts of the network is enabled and reliability indices are calculated. Figure 6 depicts the improvement of system reliability indices when the DR potential of customers connected to either main feeder or laterals is activated. As can be seen, enabling DR potential of customers hosted by laterals is more effective in improving system reliability indices.

Figure 7 compares the improvement of system reliability indices when customers in either the upper half or lower half of the network are participated in the DR program. As can be seen, DR from customers connected to the ending part of the network is more effective in improving system reliability indices.

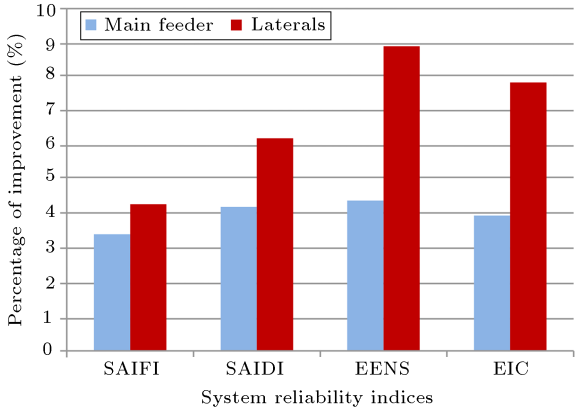

Figure 6. Comparison of system reliability improvement for customers placed at the main feeders and laterals.

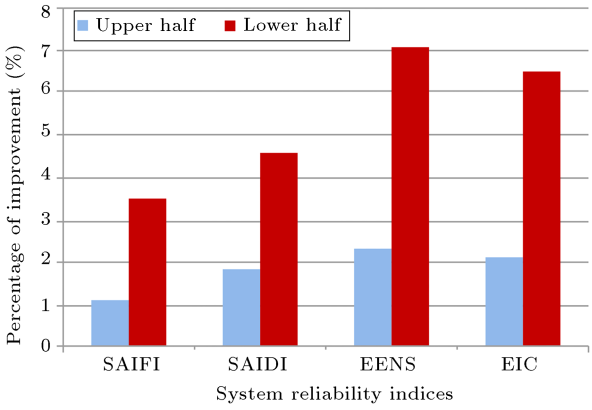

Figure 7. Comparison of system reliability improvement for customers placed at the beginning and ending part of feeder.

5. Conclusion

This paper presented a centralized scheme to coordinate residential Demand Response (DR) potentials in order to improve the reliability of the distribution

system. The model enjoyed flexible operation of responsive appliances and Plugged-in Hybrid Electric Vehicles (PHEVs) to meet violations of network operational constraints and avoid costly load curtailments. The proposed model adhered to customers' preferences since the operation of responsive loads was adjusted within the bounds and limits defined by the owners. The model was applied to a real-world distribution network with several customers. The conducted studies demonstrated the effectiveness of the model in enhancing all service reliability indices. It was shown that the improvement was achieved through negligible adjustments in the operation of responsive loads. It was determined that customers connected to the main feeders and lower half of the network experienced more significant benefits from the DR program. Also, it was demonstrated that the DR potential of customers connected to the laterals and lower half of the network was more effective in improving the system reliability.

Indices (Sets)

$n(N)$	Index(set) of responsive customers
$t(T)$	Index(set) of time intervals
$k(K)$	Index(set) of time intervals of appliance's energy consumption profile
$a(A)$	Index(set) of responsive appliances
$b, b'(B)$	Indices(set) of network buses
$c(C)$	Index(set) of contingencies
NB	Set of responsive loads at each bus of the network
NP	Set of customers with plugged-in hybrid electric vehicle

Constants and parameters

$P^{n,t}_{fixed}$, $Q^{n,t}_{fixed}$	Non-responsive part of active and reactive powers associated with responsive customer n at time step t
k_a	Number of required time steps for complete operation of appliance a
p^k_a	Active power demand of appliance a at time step k of its ECP
α^n_a, β^n_a	Beginning/end of allowable period for the operation of appliance a of customer n
α^n_{PHEV}, β^n_{PHEV}	Arrival/departure times of the nth customer's PHEV
E^n_{0p}	Primary charging level of the nth customer's PHEV at the arrival time
E^n_p	The nth customer's PHEV energy consumption during out-of-home period
$\overline{E}^n_p$	Battery capacity of the customer's PHEV
$\overline{E}^n_{ch\_p}, \underline{E}^n_{ch\_p}$	Maximum/minimum charging rate of PHEV's battery
$\overline{E}^n_{dch\_p}, \underline{E}^n_{dch\_p}$	Maximum/minimum discharging rate of PHEV's battery
$P^{b,t}_{NR}$, $Q^{b,t}_{NR}$	Active/reactive power demands of non-responsive loads at bus b and time step t
$PQR^{n,t}_R$	Active to reactive powers ratio of responsive customers
$PQR^{b,t}_{NR}$	Active to reactive powers ratio of non-responsive customers
$PQR^{n,t}_{PHEV}$	Active to reactive powers ratio of PHEV's battery charger
PF^t_{sys}	Power factor of distribution network at time step t
$\overline{V}, \underline{V}$	Upper/lower allowed voltage amplitude
$G_{b,b'}$, $B_{b,b'}$	Real/imaginary parts of the respective element in the admittance matrix
$\overline{S}_{b,b'}$	Capacity of the line from bus b to b'
$L^t_{b,b'}$	Binary variable indicating up or down state of line from bus b to b' at time step t
$VOLL_b$	Value Of Lost Load (VOLL) at bus b
$\eta^n_{ch\_p}, \eta^n_{dch\_p}$	Charging and discharging efficiencies of the nth PHEV's battery.

Functions and variables

TIC	Total interruption cost associated with load curtailments
$P^{n,t}_a, Q^{n,t}_a$	Active/reactive power demands of the nth customer's appliance a at time t
$z^{n,t}_a$	Binary variable indicating startup status of the nth customer's appliance a at time step t; 1 if the appliance is started up, 0 otherwise
$x^{n,t}_{ch\_p}$, $x^{n,t}_{dch\_p}$	Charging/discharging binary indicators of the nth customer's PHEV at time step t
$P^{n,t}_{ch\_p}, Q^{n,t}_{ch\_p}$	Active/reactive charging rates of the nth customer's PHEV battery at time step t
$P^{n,t}_{dch\_p}, Q^{n,t}_{dch\_p}$	Active/reactive discharging rates of the nth customer's PHEV battery at time step t
$E^{n,t}_{ch\_p}, E^{n,t}_{dch\_p}$	Charging/discharging energies of the nth customer's PHEV at time step t
$PF^t_{b,b'}$, $QF^t_{b,b'}$	Active/reactive power flows of line between bus b to b' at time step t

$PC_{NR}^{b,t}, QC_{NR}^{b,t}$	Active/reactive loads curtailed from non-responsive loads at bus b and time step t
$PC_{R}^{n,t}, QC_{R}^{n,t}$	Active/reactive loads curtailed from the nth customer's responsive load at time step t
$V_{b,t}, \delta_{b,t}$	Amplitude and phase angle of voltage at bus b and time step t

Acknowledgment

The authors would like to thank the Iran National Science Foundation (INSF) for its supports.

References

1. Escalera, A., Hayes, B., and Prodanović, M. "A survey of reliability assessment techniques for modern distribution networks", *Renewable and Sustainable Energy Reviews*, **91**, pp. 344–357 (2018).
2. Ravaghi Ardabili, H.A., Haghifam, M.R., and Abedi, S.M. "A probabilistic reliability-centered maintenance approach for electrical distribution networks", *IET Generation, Transmission and Distribution*, **15**(2), pp. 1070–1080 (2021). DOI: 10.1049/gtd2.12081
3. Arefi, A., Ledwich, G., Nourbakhsh, G., et al. "A fast adequacy analysis for radial distribution networks considering reconfiguration and DGs", *IEEE Transactions on Smart Grid*, **11**(5), pp. 3896–3909 (2020).
4. Davarzani, S., Pisica, I., Taylor, G.A., et al. "Residential demand response strategies and applications in active distribution network management", *Renewable and Sustainable Energy Reviews*, **138**, pp. 110567–110609 (2021).
5. Lee, M., Aslam, O., Foster, B., et al. " Assessment of demand response and advanced metering", Federal Energy Regulatory Commission, Tech. Rep. (2013).
6. Todd, D., Caufield, M., Helms, B., et al. "Providing reliability services through demand response: A preliminary evaluation of the demand response capabilities of Alcoa Inc", ORNL/TM, **233**, pp. 1–52 (2008).
7. Wang, Y., Rahimi Pordanjani, I., and Xu, W. "An event-driven demand response scheme for power system security enhancement", *IEEE Transactions on Smart Grid*, **2**(1), pp. 23–29 (2011).
8. Safdarian, A., Lehtonen, M., Fotuhi-Firuzabad, M., et al. "Customer interruption cost in smart grids", *IEEE Transactions on Power Systems*, **29**(2), pp. 994–995 (2014).
9. Goel, L., Wu, Q., and Wang, P. "Reliability enhancement of a deregulated power system considering demand response", *Proc. IEEE Power Engineering Society General Meeting*, Montreal, Que, pp. 6–11 (2006).
10. Mohagheghi, S., Yang, F., and Falahati, B. "Impact of demand response on distribution system reliability", *Proc. IEEE Power Engineering Society General Meeting*, San Diego, CA, pp. 1–7 (2011).
11. Safdarian, A., Degefa, M.Z., Lehtonen, M., et al. "Distribution network reliability improvements in presence of demand response", *IET Generation, Transmission and Distribution*, **8**(12), pp. 2027–2035 (2014).
12. Pourghaderi, N., Fotuhi-Firuzabad, M., Kabirifar, M., et al. "Reliability-based optimal bidding strategy of a technical virtual power plant", *IEEE Systems Journal*, **16**(1), pp. 1080–1091 (2021).
13. Safdarian, A., Fotuhi-Firuzabad, M., and Lehtonen, M. "Demand response from residential consumers: potentials, barriers, and solutions", *Smart Grids and Their Communication Systems*, Springer, Singapore, pp. 255–279 (2019).
14. Moradzadeh, B. and Tomsovic, K. "Two-stage residential energy management considering network operational constraints", *IEEE Transactions on Smart Grid*, **4**(4), pp. 2339–2346 (2013).
15. Zhang, C., Xu, Y., Dong, Z.Y., et al. "Robust coordination of distributed generation and price-based demand response in microgrids", *IEEE Transactions on Smart Grid*, **9**(5), pp. 4236–4247 (2017).
16. Safdarian, A., Fotuhi-Firuzabad, M., and Lehtonen, M. "Optimal residential load management in smart grids: A decentralized framework", *IEEE Transactions on Smart Grid*, **7**(4), pp. 1836–1845 (2015).
17. Safdarian, A., Ali, M., Fotuhi-Firuzabad, M., et al. "Domestic EWH and HVAC management in smart grids: Potential benefits and realization", *Electric Power Systems Research.*, **134**, pp. 38–46 (2016).
18. Chang, T., Alizadeh, M., and Scaglione, A. "Real-time power balancing via decentralized coordinated home energy scheduling", *IEEE Transactions on Smart Grid*, **4**(3), pp. 1490–1504 (2013).
19. de Souza Dutra, M.D. and Alguacil, N. "Optimal residential users coordination via demand response: An exact distributed framework", *Applied Energy*, **279**, pp. 115851–115861 (2020).
20. Kou, X., Li, F., Dong, J., et al. "A distributed energy management approach for residential demand response", *2019 3rd International Conference on Smart Grid and Smart Cities (ICSGSC)*, pp. 170–175 (2019).
21. Stamminger, R. "Synergy potential of smart appliances", *EIE, D2.3 of WP 2 from the Smart-A Project* (2008).
22. Kabirifar, M., Pourghaderi, N., Rajaei, A., et al. "Deterministic and probabilistic models for energy management in distribution systems", *Handbook of Optimization in Electric Power Distribution Systems*, pp. 343–383 (2020).
23. Corchero, C., Cruz-Zambrano, M., and Heredia, F.J. "Optimal energy management for a residential microgrid including a vehicle-to-grid system", *IEEE Transactions on Smart Grid*, **5**(4), pp. 2163–2172 (2014).

24. '2017 National household travel survey, U.S. Transportation Department", [Online]. Available: https://nhts.ornl.gov/assets/2017_nhts_summary_travel_trends.pdf.

25. Safdarian, A., Fotuhi-Firuzabad, M., and Aminifar, F. "A novel efficient model for power flow analysis of power systems", *Turk. J. Elec. Eng. Comp. Sci.*, **23**(1), pp. 52–66 (2015).

26. Billinton, R. and Allan, R.N., *Reliability Evaluation of Power Systems*, Plenum, New York (1996).

27. The IBM ILOG CPLEX Website, [Online]. Available: http://www-01.ibm.com/software/commerce/optimization/cplex-optimizer.

28. Disaggregated load data of case study, [Online]. Available: https://drive.google.com/file/d/1ZrvRzVbKl5Ea HtzfhIFLP8M5g6c1ew89/view?usp=sharing.

29. Ruiz, V. "Standards for the performance and durability assessment of electric vehicle batteries", JRC Technical Reports (2018).

30. Kisacikoglu, M.C., Bedir, A., Ozpineci, B., et al. "PHEV-EV charger technology assessment with an emphasis on V2G operation", Oak Ridge Nat. Lab., Oak Ridge, TN, USA, Tech. Rep. ORNL/TM-2010/221 (2012).

31. Mongird, K., Viswanathan, V., Alam, J., et al. "2020 grid energy storage technology cost and performance assessment", PNNL Report (2020).

Appendix

In this section, the input data of the model are presented. Three main categories of input data including load and customers' data, network data, and reliability data are presented in this section.

There are 61 load points and total 200 residential customers in the network under study. The peak load and number of the customers at each load point are summarized in Table A.1. The customers' load data are related to the finnish network, which is available for weekdays and weekends through 4 seasons of the year. For reproducibility purposes, disaggregated load data that show the electric appliances consuming power in each time step can be downloaded from [28]. The load data are related to a typical customer and the fix load of a typical customer is extracted by considering the consumed power of non-responsive appliances. In addition, the fix loads of 200 customers in the network were generated considering the typical load profile and using Monte-Carlo simulation by adopting normal probability distribution function with a standard deviation of 10%. A sample load profile for a weekday in the summer is depicted in Figure A.1.

The consumption patterns of responsive appliances are taken from [28] and [21]. The starting time and end time of each appliance operation are achieved

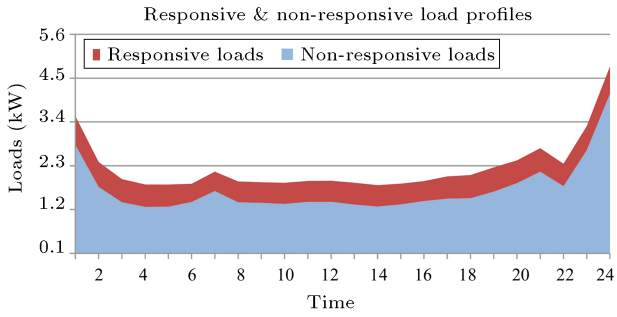

Figure A.1. Typical load profile of a customer in a weekday at summer.

based on the responsive load profiles in Finland and allowable delay that each customer is ready to apply in its utilization plan. Based on the data presented in [28], the preferred start time of each responsive appliance is obtained and using Monte-Carlo simulation, the preferred starting time of each responsive appliance is generated for each responsive customer. The average delay in the utilization of each appliance is obtained based on the statistical data presented in [21]. For example, the applied delay in using washing machine is presented in Figure A.2. The data related to Finland are used to estimate the allowable delay time.

The penetration level of PHEVs is assumed to be 15%. Based on [29] and [30], charging/discharging rate limits of PHEV battery are assumed to be 3 kWh. In addition, the rate of charging/discharging efficiency is assumed to be 0.9. The capacity of PHEVs batteries is randomly selected based on PNNL report [31]. The arrival and departure times of vehicles to/from the home are generated based on the historical data presented by NHTS [24] using stochastic method.

The distribution network under study is a real-world network located in Finland, which is depicted in Figure 5. As depicted, this network feeds 61 load points through 2 radial feeders with a normally open tie line between them. The tie-line switch and four circuit breakers C1–C4 enable reconfiguring the network topology following fault occurrence in the network. The technical data of the network are summarized in Table A.1 and Table A.2. The nominal voltage of the network is 20 kV and the allowable bound of nodes' voltage magnitude is $[0.95 - 1.05]$ p.u.

The data required for reliability assessment is another set of input data. The VOLL of load points as well as peak load and number of customers are presented in Table A.1. The availability of network branches is presented in Table A.2. The repair time of the branches and switching time are assumed to be equal to 6 hours and 1 hour, respectively. The branches' failure rates are determined by the availability and repair time data. In order to calculate the reliability indices, the proposed model is run for

Table A.1. Peak demand, number of customers, and VOLL of load points.

Bus #	Apparent peak load (kVA)	Active peak load (kW)	Number of customers	VOLL ($/kWh)	Bus #	Apparent peak load (kVA)	Active peak load (kW)	Number of customers	VOLL ($/kWh)
1	24.2	22.99	1	10.4	32	58.6	55.67	4	17.9
2	11.8	11.21	3	29.9	33	86.3	81.985	4	23.3
3	11.4	10.83	1	24.5	34	89	84.55	7	24.5
4	38	36.1	3	29.9	35	10.2	9.69	1	19.2
5	6.07	5.7665	1	24.5	36	81.4	77.33	5	15.9
6	71.4	67.83	3	26.7	37	102	96.9	6	24.5
7	58.5	55.575	4	24.5	38	38.6	36.67	4	60
8	34.9	33.155	4	24.5	39	0.73	0.6935	0	24.5
9	7.36	6.992	1	24.5	40	95.1	90.345	6	16.1
10	50.3	47.785	2	29.9	41	56.4	53.58	4	33.8
11	124	117.8	7	10.2	42	30.9	29.355	2	29.9
12	29.7	28.215	2	18.1	43	22.7	21.565	1	33.8
13	39.3	37.335	3	29.9	44	6.11	5.8045	2	10.4
14	55.4	52.63	2	29.9	45	49.9	47.405	6	24.5
15	87.8	83.41	5	24.5	46	35.3	33.535	4	29.9
16	53.7	51.015	4	15.1	47	27.6	26.22	3	24.5
17	63.6	60.42	3	27.8	48	31.5	29.925	2	27.9
18	22.3	21.185	1	26.3	49	55.6	52.82	5	19.2
19	50.2	47.69	5	24.1	50	3.31	3.1445	2	28.5
20	15.4	14.63	0	24.5	51	68.6	65.17	3	24.8
21	24.4	23.18	1	15.8	52	24	22.8	1	33.1
22	37.3	35.435	5	24.5	53	143	135.85	7	24.5
23	120	114	4	16	54	83	78.85	3	12.8
24	49.9	47.405	6	29.9	55	32	30.4	1	17.9
25	23.7	22.515	1	7.86	56	78.2	74.29	2	29.9
26	42.2	40.09	4	29.9	57	32.1	30.495	2	14
27	34.4	32.68	4	29.9	58	40	38	4	25.1
28	31.8	30.21	4	31.1	59	38.5	36.575	1	24.5
29	99.4	94.43	5	24.5	60	7.1	6.745	1	29.9
30	43.5	41.325	6	15.3	61	99.1	94.145	6	28.3
31	85.8	81.51	5	29.9	–	–	–	–	–

Table A.2. Network line data including technical and availability data.

Line #	FB	TB	R (Ω)	X (Ω)	Cap (kVA)	Availability	Line #	FB	TB	R (Ω)	X (Ω)	Cap (kVA)	Availability
1	0	1	0.8463	0.3973	800	0.999997	32	31	32	1.3918	0.4074	200	0.999995
2	1	2	0.4124	0.1936	800	0.999987	33	0	33	0.3749	0.1760	800	0.999996
3	2	3	0.1884	0.0884	800	0.999995	34	33	34	0.3401	0.1597	800	0.999996
4	3	4	0.0100	0.0047	800	0.999996	35	34	35	0.3486	0.1020	200	0.999987
5	4	5	0.7811	0.2286	200	0.999995	36	34	36	0.1048	0.0492	800	0.999996
6	4	6	0.1645	0.0772	800	0.999996	37	36	37	0.3761	0.1101	200	0.999991
7	6	7	0.2699	0.1267	800	0.999995	38	36	38	0.1216	0.0571	800	0.999992
8	7	8	0.2754	0.1293	800	0.999992	39	38	39	0.1860	0.0873	800	0.999994
9	8	9	0.2306	0.1082	800	0.999994	40	39	40	0.2494	0.1171	800	0.999998
10	9	10	0.7365	0.2156	800	0.999991	41	40	41	0.4433	0.1298	200	0.999995
11	10	11	0.5141	0.1505	800	0.999996	42	41	42	1.0350	0.3029	200	0.999996
12	10	12	0.2196	0.0643	200	0.999999	43	42	43	0.5182	0.1517	200	0.999994
13	12	13	0.5881	0.1721	200	0.999994	44	43	44	0.3811	0.1115	200	0.999998
14	13	14	0.2526	0.0739	200	0.999997	45	44	45	0.3847	0.1126	200	0.999993
15	13	15	0.5272	0.1543	200	0.999995	46	45	46	0.4190	0.1226	200	0.999997
16	9	16	0.1420	0.0667	800	0.999998	47	46	47	0.4253	0.1245	200	0.999998
17	16	17	0.1459	0.0685	800	0.999998	48	47	48	0.8524	0.2495	200	0.999996
18	17	18	0.4808	0.1407	200	0.999997	49	40	49	0.5164	0.1511	200	0.999997
19	18	19	0.3076	0.0900	200	0.999993	50	49	50	0.9119	0.2669	200	0.999996
20	19	20	0.3184	0.0932	200	0.999995	51	50	51	0.6314	0.1848	200	0.999998
21	20	21	0.4339	0.1270	200	0.999998	52	51	52	0.6355	0.1860	200	0.999995
22	21	22	0.4943	0.1447	200	0.999997	53	52	53	0.9832	0.2878	200	0.999994
23	21	23	0.4312	0.1262	200	0.999997	54	51	54	0.9588	0.2806	200	0.999994
24	23	24	0.3788	0.1109	200	0.999997	55	40	55	0.4194	0.1228	200	0.999997
25	24	25	0.5132	0.1502	200	0.999996	56	55	56	0.4496	0.1316	200	0.999995
26	17	26	0.5638	0.1650	200	0.999997	57	56	57	0.5380	0.1575	200	0.999997
27	26	27	0.2426	0.0710	200	0.999996	58	56	58	0.4325	0.1266	200	0.999996
28	27	28	0.3342	0.0978	200	0.999995	59	58	59	0.0753	0.0220	200	0.999996
29	28	29	0.4596	0.1345	200	0.999996	60	56	60	0.6386	0.1869	200	0.999997
30	26	30	0.3148	0.0921	200	0.999994	61	60	61	0.6693	0.1959	200	0.999996
31	30	31	0.6120	0.1791	200	0.999991	62	30	61	0.3784	0.1107	200	0.999997

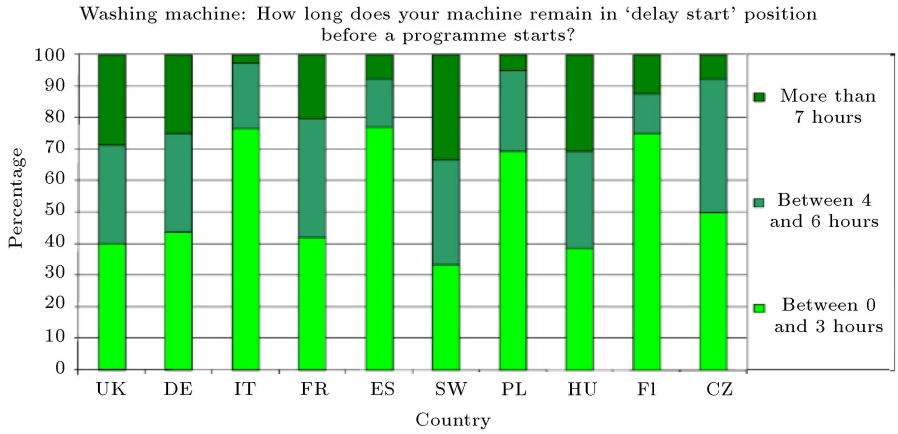

Figure A.2. Applied delay in using washing machine by customers [21].

8 days (for each season, 2 days are considered, one for weekdays and another for weekends). The time set for each day is equal to $1, 2, 3, \cdots, 96$ and the duration of each time interval is equal to 0.25 hours.

Biographies

Milad Kabirifar received the BSc degree from Isfahan University of Technology, Isfahan, Iran in 2014 and the MSc degree in Electrical Engineering from Sharif University of Technology, Tehran, Iran in 2016, where he is currently pursuing the PhD degree. His current research interests include distribution network operation and planning, power system reliability, and optimization of smart electricity grids.

Mahmud Fotuhi-Firuzabad received the BSc degree from the Sharif University of Technology, Tehran, Iran in 1986, the MSc degree from Tehran University in 1989, and the MSc and PhD degrees from the University of Saskatchewan, Canada in 1993 and 1997, respectively, all in Electrical Engineering. He is currently a Professor at the Electrical Engineering Department and the President of the Sharif University of Technology. He is a member of the Center of Excellence in Power System Control and Management at the Electrical Engineering Department. He is also a Visiting Professor with Aalto University, Finland. His research interests include power system reliability, distributed renewable generation, demand response, and smart grids. He is a recipient of several national and international awards including the World Intellectual Property Organization (WIPO) Award for the Outstanding Inventor, 2003, and the PMAPS International Society Merit Award for contributions of probabilistic methods applied to power systems in 2016. He serves as the Editor-in-Chief of the IEEE Power Engineering Letters.

Amir Safdarian has been a Faculty Member at Sharif University of Technology, Iran since 2015. He has extensive teaching and research experience. His research interests include electric power distribution system operation and planning, smart grid related issues, and energy system reliability and resilience. He was a recipient of several national and international awards, including the 2013 IEEE Power System Operation Transactions Prize Paper Award. He was on the list of outstanding reviewers of IEEE Transactions on Sustainable Energy for 2016. Since 2019, he has been an Associate Editor of IET Generation, Transmission and Distribution.